Published in final edited form as:
Cell Metab. 2008 April ; 7(4): 302–311. doi:10.1016/j.cmet.2008.03.003.

Hepatic steatosis in leptin-deficient mice is promoted by the PPARγ target gene, fat-specific protein 27

Kimihiko Matsusue[1,2], **Takashi Kusakabe**[3], **Takahiro Noguchi**[2], **Shouichi Takiguchi**[4], **Toshimitsu Suzuki**[3], **Shigeru Yamano**[2], and **Frank J. Gonzalez**[1]

1*Laboratory of Metabolism, National Cancer Institute, National Institutes of Health, Bethesda, Maryland 20892*

2*Faculty of Pharmaceutical Science, Fukuoka University, 8−19−1 Nanakuma, Jonan-ku, Fukuoka 814−0180, Japan.*

3*Department of Pathology, Fukushima Medical University School of Medicine, Fukushima, Japan.*

4*Institute for Clinical Research, National Kyushu Cancer Center, 3−1−1 Notame, Minami-ku, Fukuoka 811−1395, Japan*

Summary

PPARγ is induced in leptin-deficient mouse (*ob/ob*) liver and is critical for the development of hepatic steatosis. The present study shows that *fsp27* in *ob/ob* liver is a direct target gene of PPARγ and can elevate hepatic triglyceride levels. Fsp27 belongs to the cide family, composed of cide a, cide b and fsp27/cide c, that all contain a conserved CIDE-N domain. Fsp27 was recently reported to be a lipid droplet-binding protein and to promote lipid accumulation in adipocytes. The *fsp27* gene was expressed at high levels in *ob/ob* liver, and at markedly lower levels in *ob/ob* livers lacking PPARγ. Forced expression of fsp27 by adenovirus, in hepatocytes *in vitro* or *in vivo*, led to increased triglyceride levels. Knockdown by adenovirus expressing fsp27-shRNA resulted in lower accumulation of hepatic triglycerides compared to control adenovirus-infected liver. Taken together, these results indicate that the fsp27 is a direct mediator of PPARγ-dependent hepatic steatosis.

Keywords

PPAR; PPARgamma; fsp27; cide; triglyceride; knockout mouse; fatty liver; ob/ob

Introduction

Peroxisome proliferator-activated receptors γ (PPARγ) belongs to the nuclear receptor superfamily and can regulate the transcription of genes in response to specific ligands. The synthetic ligands of PPARγ, thiazolidinediones, are clinically used to reduce insulin resistance and improve hyperglycemia associated with type 2 diabetes (Gervois et al., 2007). PPARγ is expressed at the highest level in adipose tissue (Tontonoz et al., 1994) and is required for the differentiation of pre-adipocytes to mature adipocytes (Rosen et al., 2002). In contrast, PPARγ is normally expressed in both human and murine livers at only 10−30% of the levels found in adipose tissue (Tontonoz et al., 1994). However, PPARγ is expressed at markedly

Corresponding author: Kimihiko Matsusue, Faculty of Pharmaceutical Science, Fukuoka University, 8−19−1 Nanakuma, Jonan-ku, Fukuoka 814−0180, Japan. Email: matsusuk@fukuoka-u.ac.jp.

Shigeru Yamano and Frank J. Gonzalez contributed equally to this work

elevated levels in the severe fatty livers associated with a number of murine models of diabetes or obesity (Bedoucha et al., 2001; Memon et al., 2000).

Previously, a PPARγ-liver null mouse on an *ob/ob* background (*ob/ob*-PPARγ/Cre$^+$) was generated using a floxed PPARγ allele and Cre recombinase under control of the albumin promoter. The *ob/ob*-PPARγ/Cre$^+$ mouse showed a marked decrease in hepatic triglyceride content and improvement of fatty liver compared to equivalent mice lacking the Cre transgene (*ob/ob*-PPARγ/Cre$^-$) (Matsusue et al., 2003). These results strongly suggest that PPARγ is capable of activating the expression of genes involved in triglyceride accumulation in hepatocytes and promoting the generation of fatty liver. However, the molecular mechanism and downstream target genes of hepatic PPARγ associated with hepatic steatosis remain largely unknown.

To enhance the current understanding of the mechanism of PPARγ-dependent fatty liver formation, studies were performed to identifying downstream target genes of hepatic PPARγ, by use of subtractive cDNA cloning between *ob/ob*-PPARγ/Cre$^-$ and/Cre$^+$ livers. The *fsp27* gene was identified as a fatty liver-specific gene and a direct downstream target of hepatic PPARγ. In addition, forced expression of fsp27 by adenovirus in hepatocytes *in vivo* and *in vitro* results in an increase in lipid droplets through elevation of triglyceride levels while knockdown of fsp27 in *ob/ob* mice resulted in loss of hepatic lipid.

Results

Identification of transcriptional target of hepatic PPARγ by subtraction screening

To identify direct transcriptional targets of hepatic PPARγ in *ob/ob* mouse fatty liver, a subtractive cloning strategy was used that takes advantage of the availability of the liver-specific PPARγ-null mouse and the specificity provided by the synthetic PPARγ ligand, rosiglitazone. RNA from *ob/ob*-PPARγ/Cre$^-$ and Cre$^+$ livers was used to create a subtracted cDNA library and after accounting for redundancy, only three cDNAs were identified from the screening as being specifically expressed in *ob/ob* mouse fatty liver; stearoyl-CoA desaturase-1 (SCD-1), fat specific protein 27 (fsp27) and cell death-inducing DFFA-like effector a (cide a).

A decrease in SCD-1 mRNA in PPARγ-null ob/ob liver was previously demonstrated (Matsusue et al., 2003). The *cide a* and *fsp27* genes are members of the cide family (Lin and Li, 2004). Rat *CIDE A* was originally identified as a gene encoding a protein with homology to the N-terminal region of DNA fragmentation factor 45. Overexpression of CIDE A in 293T cells led to enhanced apoptosis (Inohara et al., 1998). Independently, the *fsp27* was isolated as a gene specifically expressed in the fully differentiated mouse adipocyte cell line, TA1 (Danesch et al., 1992; Williams et al., 1992). The human ortholog of *fsp27* gene, referred to as *CIDE 3*, also induced apoptosis (Liang et al., 2003). To determine the molecular mechanism for development of PPARγ-dependent hepatic steatosis, the physiological role of the *cide a* and *fsp27* gene products in fatty liver was examined.

Expression of the cide a and fsp27 genes depends on fatty liver formation and hepatic PPARγ expression

The mouse cide family is composed of three genes, *cide a*, *cide b* and *fsp27* (Inohara et al., 1998; Liang et al., 2003). The expression of these genes on *ob/ob*-PPARγ/Cre$^-$ or *ob/ob*-PPARγ/Cre$^+$ mouse livers was confirmed by Northern blotting (Figure 1). Expression of the *cide a* and *fsp27* mRNAs was observed in *ob/ob*-PPARγ/Cre$^-$ liver. However, they were expressed at markedly lower levels in *ob/ob*-PPARγ/Cre$^+$ liver and not detectable in livers from normal genetic background, *OB/OB*-PPARγ/Cre$^-$ and *OB/OB*-PPARγ//Cre$^+$ mice.

Rosiglitazone treatment induced the expression of *cide a* and *fsp27* mRNAs in *ob/ob*-PPARγ/Cre$^-$ mouse liver but not in *ob/ob*-PPARγ/Cre$^+$ mouse liver. In contrast to the selective expression of the *cide a* and *fsp27* genes, the *cide b* gene was highly expressed in all livers of the mouse lines examined with no response to the hepatic PPARγ deficiency or rosiglitazone treatment noted. Since hepatic steatosis develops on the *ob/ob*-PPARγ/Cre$^-$ mouse background and is improved by disrupting PPARγ expression in this tissue, these results indicate that expression of the *cide a* and *fsp27* genes is hepatic PPARγ-dependent and positively correlated with development of hepatic steatosis.

PPARγ-dependent cide a and fsp27 expression does not induce apoptosis in ob/ob mouse liver

The *cide a* and *fsp27* genes are highly expressed in *ob/ob*-PPARγ/Cre$^-$ liver but not in *ob/ob*-PPARγ/Cre$^+$ liver (Figure 1). An earlier report demonstrated that overexpression of rat CIDE A in a cell line induces apoptosis (Inohara et al., 1998). Thus, to compare apoptosis between *ob/ob*-PPARγ/Cre$^-$ and *ob/ob*-PPARγ/Cre$^+$ livers, TUNNEL assay was performed in liver sections from both mice. However, no significant difference in apoptosis was observed between *ob/ob*-PPARγ/Cre$^-$ and *ob/ob*-PPARγ/Cre$^+$ mouse livers (data not shown). These results suggest that the *cide a* and *fsp27* gene products expressed in hepatic steatosis have a physiological function in liver independent of apoptosis.

Different expression pattern of the cide a and fsp27 genes

To determine the tissue-specific expression of the *cide a and fsp27* genes, the tissue distribution of expression was studied in *ob/ob*-PPARγ/Cre$^-$ and *ob/ob*-PPARγ/Cre$^+$ mice (Supplemental Figure 1A). In addition to expression in the liver (LI), expression of the *cide a* gene was specifically observed in brown adipose (BA) and slightly induced in white adipose (W) by administration of rosiglitazone. The fsp27 gene was highly expressed in both brown (BA), white adipose (W) and liver (Ll), and expressed at lower levels in lung (L) and colon (C). Rosiglitazone also induced *fsp27* mRNA in these tissues. Expression of the *cide b* gene was observed in kidney (K), liver (LI) and colon (C) and was unchanged by rosiglitazone.

The *fsp27* gene was also expressed in the fully differentiated 3T3-L1 adipocytes in which PPARγ is highly expressed and induced by rosiglitazone treatment (Supplemental Figure 1B). Furthermore, infection of mouse primary hepatocytes with an adenovirus vector expressing PPARγ not only induced *fsp27* but also *aP2* mRNA, which is a known PPARγ-target gene (Supplemental Figure 1C). It is noteworthy that expression of the *cide a* gene was not observed under the same conditions where *fsp27* and *PPARγ* were expressed. These data suggest that the transcriptional mechanism of *cide a* differs from that of *fsp27*.

Brown adipose tissue also expressed both the *cide a* and *fsp27* genes (Supplemental Figure 1A). Thus, mouse primary brown adipocytes were used to further characterize expression of the *cide a* and *fsp27* genes. Consistent with earlier reports (Zhou et al., 2003), expression of *cide a* depends on the differentiation of adipocytes and is markedly decreased by the addition of TNFα. Although *fsp27* also showed differentiation-dependent expression, expression was less sensitive to TNFα (Supplemental Figure 2).

A functional PPRE is involved in the promoter region of fsp27 gene

Expression of the *fsp27* gene was correlated with the expression pattern of PPARγ (Figure 1). However, expression of the *cide a* gene was not correlated with PPARγ expression, suggesting the possibility of an indirect regulation by PPARγ. Thus, transcriptional regulation of the *fsp27* gene through PPARγ was investigated. By searching the database (MOTIF; http://motif.genome.ad.jp/), a putative PPRE sites in the promoter region of *fsp27* was revealed at position −214/−202 from the transcriptional start site (−1). Putative binding sites for other

transcription factors in the 5'-upstream region of the *fsp27* gene were also identified as HNF-3, GATA-3, SREBP-1, CREBP and C/EBP. To elucidate whether the *fsp27* gene PPRE is functional, reporter constructs with serially deletions of 5'-flanking DNA of *fsp27* were prepared. The activity of the luciferase reporter constructs D1 and D2 was activated by the addition of rosiglitazone, whereas constructs D3 and D4, lacking the PPRE, had completely lost the induction of activity by rosiglitazone (Figure 2A). Point mutations (mut1 and mut2) introduced into the PPRE element in the D2 construct resulted in loss of activation by rosiglitazone (Figure 2B). Further, to assess whether the luciferase construct including fsp27-PPRE is also activated by other PPAR isoforms, PPARα or PPARβ were transfected with or without their respective specific ligands, Wy-14,643 and L-165041 (Figure 2C). The luciferase activity of a positive control construct driving by the thymidine kinase promoter including the consensus PPRE was markedly induced by these ligands in the presence of each PPAR isoform (Figure 2C, left panel). However, under the same conditions, PPARα and PPARβ could not induce the activity of the fsp27-PPRE, while PPARγ significantly induced the activity of this construct (Figure 2C, right panel). These results suggest that the PPRE (−214/−202) identified on the *fsp27* promoter is a functional and PPARγ-specific *cis*-element.

Endogenous PPARγ in 3T3-L1 adipocytes or ob/ob fatty liver directly interact with fsp27-PPRE

To demonstrate additional evidence for direct regulation by PPARγ, an electrophoretic mobility shift assays (EMSA) using fsp27-PPRE as probe was performed (Supplemental Figure 3). PPARα/RXRα or PPARγ/RXRα heterodimers were formed when the consensus PPRE probe was used. Similarly, the aP2-PPRE probe was observed to bind with both PPARs/RXRα heterodimers under the present conditions. The RXRα/RXRα homodimers could also bind to these probes (Vivat-Hannah et al., 2003). Interestingly, PPARγ/RXRα heterodimers could bind to the fsp27-PPRE probe while the PPARα/RXRα heterodimers exhibited much weaker binding. These results suggest that PPARγ can directly bind to the fsp27-PPRE and the binding is likely to be of high affinity for PPARγ as supported by the data in Figure 2C.

To demonstrate an interaction between endogenous PPARγ and fsp27-PPRE under physiological conditions, a chromatin immunoprecipitation (ChIP) assay was performed with chromatin from 3T3-L1 adipocytes. Three primer sets were designed to amplify fsp27-PPRE, non-PPRE as negative control (Figure 3A) and aP2-PPRE as a positive control. The results revealed an association of endogenous PPARγ with the fsp27- or aP2-PPREs, but not with the non-PPRE. No difference in association was observed with or without rosiglitazone (Figure 3B). Next, chromatin from in *ob/ob* liver was subjected to ChIP assay. The PPARγ protein expressed in fatty liver of *ob/ob* mouse was clearly bound to the fsp27-PPRE although background weak amplification of the non-PPRE was observed (Figure 3C). Thus, these results suggest that endogenous PPARγ can also bind to fsp27-PPRE in both mature adipocytes and *ob/ob* mouse liver.

In vitro and vivo overexpression of fsp27 leads to triglyceride accumulation

To elucidate the physiological function of *fsp27* and *cide a* gene products, adenovirus vectors expressing HA-tagged fsp27 (Adfsp27) and *cide a* (Adcide a) gene products were generated. The expression of proteins was verified with the expected molecular size in each adenovirus-infected hepatocyte (Figure 4A). On examination by phase-contrast microscopy, the morphologic differences between AdLacZ- and Adfsp27-infected hepatocytes were obvious. Adfsp27-infected hepatocytes showed the generation of numerous round vacuoles in cytosolic fraction within approximately two days after infection. Further, Oil red O staining revealed fat accumulation in these vacuoles as lipid droplets (LD, Figure 4B). The LD of AdPPARγ-infected hepatocytes were much smaller and of less number than those seen in Adfsp27-infected hepatocytes. Although Adcide a-infected hepatocytes were stained by Oil red O, the

staining appears to be background as compared with that of AdlacZ. In support of the staining results, triglyceride (TG) contents in Adfsp27- and AdPPARγ-infected hepatocytes were 150% and 130% of AdLacZ-infected hepatocytes (Figure 4C). No significant difference in cholesterol content was observed between AdLacZ- and Adfsp27- or AdPPARγ-infected hepatocytes.

Previous data indicated that hepatic TG levels in *ob/ob*-PPARγ/Cre$^+$ mouse are considerably lower than in *ob/ob*-PPARγ/Cre$^-$ mice (Matsusue et al., 2003). In the present study, the *fsp27* mRNA level in *ob/ob*-PPARγ/Cre$^+$ mouse liver was also observed at lower level (Figure 1). Thus, to confirm whether the fsp27 expression is associated with decreased TG levels in *ob/ob*-PPARγ/Cre$^+$ liver, a fsp27-rescue experiment with Adfsp27 intravenously injected to *ob/ob*-PPARγ/Cre$^+$ mouse was performed. Histological analysis revealed few vacuoles in the *ob/ob*-PPARγ/Cre$^+$ mouse liver infected with AdLacZ (Figure 5A), while injection of Adfsp27 led to occurrence of numerous vacuoles (Figure 5B). However, the vacuoles were smaller than those observed in *ob/ob*-PPARγ/Cre$^-$ mouse liver (Figure 5C). The expression of HA-tagged fsp27 or LacZ proteins in these livers was verified by Western blot using HA antibody (Figure 5D). Note that in the absence of a suitable specific antibody against fsp27, we cannot precisely estimate that levels of expression of fsp27 protein produced from the recombinant adenovirus and thus cannot determine whether the levels obtained reflect the levels found in livers of ob/on mice.

The TG content of AdLacZ-infected *ob/ob*-PPARγ/Cre$^+$ liver was much lower (21% of *ob/ob*-PPARγ/Cre$^-$ liver) than that for *ob/ob*-PPARγ/Cre$^-$, but the Adfsp27-infected *ob/ob*-PPARγ/Cre$^+$ liver revealed partially recovery of the hepatic TG (40% of *ob/ob*-PPARγ/Cre$^-$ liver) (Figure 5E). These results strongly suggest that the expression of fsp27 leads to promotion of the formation of intracellular LD through the TG accumulation in *in vitro* and *in vivo* hepatocytes.

Knockdown of fsp27 partially improves the ob/ob mouse fatty liver

To determine the *in vivo* hepatic function of fsp27, a recombinant adenovirus expressing a short hairpin RNA (shRNA) targeting fsp27 was generated. An efficient shRNA sequence for silencing of fsp27-HA protein expression was selected from three candidates (Figure 6A). Since the construct 2 (lane 3) almost completely repressed fsp27-HA protein expression, it was used for the generation of the recombinant adenovirus shRNA. The adenovirus expressing fsp27shRNA (Adshfsp27) and control scramble shRNA (Adshscram) were infected to 3T3-L1 adipocytes, which constitutively express fsp27 (Figure 6B). Although adenovirus is known to have low transduction efficiency for adipocytes, the Adshfsp27 dramatically decreased *fsp27* mRNA by 35% at an 8000 MOI as compared with Adshscram, indicating that the generated Adshfsp27 is functional for knockdown of native *fsp27*. Therefore, Adshfsp27 or Adshscram was injected to the *ob/ob*-PPARγ/Cre$^-$ mouse (Figure 6C). Liver sections from the Adshscram-infected *ob/ob*-PPARγ/Cre$^-$ mouse revealed the presence of numerous and large hepatocyte vacuoles. Interestingly, the vacuoles in hepatocytes around the large vein in Adshfsp27-infected liver were clearly smaller and less numerous than those in hepatocytes remote from the vein (arrow head) although some vacuoles still remained. The Adshfsp27 dramatically decreased *fsp27* mRNA in *ob/ob*-PPARγ/Cre$^-$ mouse livers by 10% as compared with Adshscram, indicating that the generated Adshfsp27 is a functional for knockdown of native fsp27 (Figure 6D). The TG content of Adshfsp27-infected liver showed a tendency toward lower levels as compared to those of Adshscram-infected liver although there was no significant difference between Adshscram- and Adshfsp27-infected livers (Figure 6E).

Fsp27 protein in primary hepatocytes represses mitochondrial β-oxidation activity and decreases triglyceride turnover

To elucidate mechanism of TG accumulation by fsp27 protein, the metabolic profile of ^{14}C-oleic acid (OA) as TG precursor was compared between AdLacZ- and Adfsp27-infected hepatocytes. The OA uptake into hepatocytes, TG export into medium and *de novo* TG synthesis from OA were unchanged in AdLacZ- and Adfsp27-infected hepatocytes (Figure 7A-C). However, the total β-oxidation activity in Adfsp27-infected hepatocytes was significantly decreased by 65% as compared with AdLacZ (Figure 7D). The β-oxidation of fatty acid in hepatocytes occurs not only in mitochondria but also in peroxisomes. To distinguish the β-oxidation activity between mitochondria and peroxisomes, activity was measured in the absence or presence of antimycin and rotenone to inhibit the mitochondrial β-oxidation (Thomas et al., 1979). The fsp27 expressed in hepatocytes significantly decreased the activity of mitochondrial β-oxidation (Figure 7E), but not peroxisomal β-oxidation (Figure 7F). Further, TG turnover as an indicator of intracellular TG accumulation was compared between AdLacZ and Adfsp27-infected hepatocytes (Figure 7G). The hepatocytes were first incubated with ^{14}C-oleic acids/BSA complex for 24 hr to generate a pool of labeled triglyceride. The supplemental ^{14}C-oleic acids/BSA were removed and the hepatocytes were infected with AdLacZ or Adfsp27 and incubated with serum free medium containing triacsin C, a fatty acyl-CoA synthetase inhibitor, to inhibit further triglyceride synthesis (Tomoda et al., 1991). The TG content in AdLacZ-infected hepatocytes was decreased by 70% at 24 hr and 60% at 48 hr from incubation start, while the content in fsp27-infected hepatocytes was almost unchanged from starting as 90% at 24 hr or 100% at 48 hr. These results suggest the possibility that the TG accumulation by fsp27 may be due to the impaired β-oxidation activity and the reduced TG turnover.

Discussion

The cide a and fsp27 genes are fatty liver-specific and PPARγ-dependent genes

The main goal of the current study was to elucidate the molecular mechanism of PPARγ-dependent hepatic steatosis. Although *cide a* and *fsp27* genes are not novel genes, the present results demonstrated for the first time that these genes are highly expressed in the fatty livers of *ob/ob* mice and expression of both mRNAs, but not the related *cide b* mRNA, were lost in *ob/ob* livers lacking PPARγ. In addition, no expression of the *cide a* and *fsp27* genes was observed in the livers of normal genetic background mice. The deficiency of PPARγ in the *ob/ob* mouse liver dramatically improved hepatic steatosis (Matsusue et al., 2003). Therefore, the *cide a* and *fsp27* genes may be directly or indirectly involved in pathways of steatosis formation.

Fsp27 is a PPARγ-target gene in hepatic steatosis of ob/ob diabetic mouse

Analysis by Northern blots revealed that expression of the *fsp27* gene was completely restricted to cells or tissues expressing PPARγ and additively induced in the presence of PPARγ ligand. Although the expression of fsp27 was also observed in lung and colon as tissues, except for adipose or fatty liver, these tissues also express PPARγ in limited cells (Mansen et al., 1996; Simon et al., 2006). Thus, the *fsp27* gene could be a direct target gene of hepatic PPARγ. Indeed, the present studies demonstrated a functional PPRE, located at positions −214/−202 from the transcription initiation site of the *fsp27* gene that directly interacts with PPARγ *in vitro* and *in vivo*. It is noteworthy that the results of reporter assays revealed PPARγ-specific activation of promoter activity. Further, the binding affinity of PPARγ to the fsp27-PPRE was markedly stronger than that of PPARα. These results suggest that the *fsp27* gene is specifically regulated by PPARγ. The finding of a PPARγ-specific gene in hepatocytes could explain the loss of the fatty liver phenotype in the *ob/ob* mouse liver lacking PPARγ, that is independent of expression of PPARα as previously reported (Matsusue et al., 2003). Thus, the loss of hepatic TG is not solely due to activation of fatty acid catabolism by PPARα.

In contrast to the *fsp27* gene, the mechanism of regulation of the *cide a* gene remains elusive. Recently, others demonstrated that *cide a* mRNA is expressed at high levels following treatment with PPARα ligands or with PPARγ overexpression and that the promoter contains a functional PPRE responsive to both these PPAR isotypes (Viswakarma et al., 2007), thus indicating that it is directly regulated by PPARγ. However, the present studies showed that *in vitro* forced expression of PPARγ to primary mouse hepatocytes induced *fsp27* or the typical PPARγ-target gene, *aP2* gene, but not the *cide a* gene. Thus, while it remains unclear whether the *cide a* gene is directly or indirectly regulated by PPARγ, the transcriptional regulation of the *cide a* gene is clearly distinct from that of the *fsp27* gene.

Fsp27 is a direct mediator of PPARγ-dependent fatty liver formation

While the mechanisms for hepatic steatosis in *ob/ob* mice are less clear, it was previously revealed that hepatic PPARγ is critical for lipogeneic gene expression and the subsequent development of fatty liver in *ob/ob* mice (Matsusue et al., 2003). In the present study, forced expression of the fsp27 protein in primary hepatocytes resulted in an increase in lipid droplets (LD) and triglycerides (TG), but not cholesterol levels. Although the expression of lipid metabolism-related genes (fatty acid synthase, CD36 and adipose differentiation-related protein) in Adfsp27-infected hepatocytes was confirmed, there was no significant difference in TG accumulation between AdLacZ- and Adfsp27-infected wild-type mouse hepatocytes (data not shown). In addition, the fsp27 protein rescued by Adfsp27 infection of *ob/ob*-PPARγ/Cre^{+} liver that lacks *fsp27* mRNA and hepatic steatosis, resulted in recovery of TG corresponding to 20% of *ob/ob*-PPARγ/Cre^{-} mouse liver. Therefore, PPARγ-dependent TG and LD accumulation might be due in part, to fsp27 that was induced in *ob/ob* fatty liver. Elevated *fsp27* mRNA was also observed in fatty liver of high fat (HF)-fed normal mice and additively induced by the administration of pioglitazone (data not shown). This is likely due to PPARγ which is also induced in HF-fed fatty liver (Inoue et al., 2005). Therefore, the increased expression of fsp27 is associated with steatosis formation and not restricted to the *ob/ob* mouse but also in HF-fed normal mice. However, it would be interesting to determine whether TG accumulation by fsp27 also requires other factors associated with type 2 diabetes or obesity found in the ob/ob mice.

In support of the data on overexpression of fsp27, fsp27 knockdown by Adshfsp27 causes the loss of hepatocyte vacuoles. In particular, the hepatocytes around the large veins in *ob/ob*-PPARγ/Cre^{-} mouse liver revealed a clear loss of the vacuoles. Since the Adshfsp27 was intravenously injected from tail vein, the fsp27 shRNA may be more highly expressed in hepatocytes near the vein and efficiently decrease fsp27. However, the TG levels decreased by Adshfsp27 infection were not significantly different from controls. This may be due to inability of the recombinant adenovirus to penetrate the whole liver. In addition, the present study suggested that fsp27 impairs the TG turnover rate resulting in accumulation of intracellular TG. Since the intracellular TG generally has a lower turnover rate, the influence of fsp27 level decreased by Adshfsp27 appears to be not immediately reflected in decreased TG levels in the acute adenovirus expression system employed in this study.

While, the LD and TG accumulations in AdPPARγ-infected hepatocytes were less than that in Adfsp27-infected hepatocytes, overexpression of PPARγ also led to induction of *fsp27* mRNA by rosiglitazone treatment. Thus, it is likely that the fsp27, introduced to the hepatocytes by AdPPARγ, is not expressed for sufficient time in culture to cause a marked accumulation of TG and LD as is found in the livers of *ob/ob* mice. This is due to the inherent short life span of primary hepatocytes. Indeed, an earlier report demonstrated that the hepatocyte cell line, AML 12 that stably expresses PPARγ, had accelerated lipid accumulation and the expression of lipogenic genes (Schadinger et al., 2005).

Fsp27 represses the mitochondrial β-oxidation activity and decreases triglyceride turnover

The present study revealed that hepatic fsp27 promotes TG accumulation by repression of mitochondrial β-oxidation activity or decreasing triglyceride turnover. Recently, others demonstrated that the fsp27 depletion in 3T3-L1 adipocytes significantly stimulated lipolysis and reduces the size of lipid droplets (LD), indicating that fsp27 negatively regulates lipolysis and promotes the TG accumulation. Further, this study revealed that fsp27 is localized to lipid droplets and not to mitochondria in 3T3-L1 adipocytes (Puri et al., 2007), although other members of CIDE family, CIDE A, CIDE B and fsp27 (CIDE C or CIDE 3, the human ortholog of fsp27) is localized to mitochondria (Chen et al., 2000; Liang et al., 2003; Zhou et al., 2003). The present results revealed that the overexpression of fsp27 in hepatocytes decreases TG turnover in the presence of triacsin C. Since the triacsin C inhibits new TG synthesis (Tomoda et al., 1991), the decreased turnover is likely to be due to repression of lipolysis. Therefore, TG accumulation by fsp27 may occur through the TG protection from constitutive lipolysis. Such a function is not unique to fsp27; perilipin A localizing to LD in adipocytes is also capable of protecting TG from the lipolysis (Brasaemle et al., 2000).

A direct link between the impaired β-oxidation and intracellular TG accumulation is less clear. However, earlier reports have revealed evidence for this association. Mitochondrial trifunctional protein (MTP) is a complex enzyme that catalyzes the final steps of mitochondrial β-oxidation. *Mtp*-null mice die at 6−36 hours after birth coincident with rapid development of hepatic steatosis (Ibdah et al., 2001). It remains unclear whether and how fsp27 suppresses β-oxidation activity. One possible mechanism may be that decreased TG turnover might be a secondary cause of impairment of β-oxidation activity due to lack of fatty acyl-CoA released from TG. The suppression mechanism by fsp27 on β-oxidation is the subject of future studies.

In a previous report, rosiglitazone markedly exacerbated hepatic steatosis in *ob/ob* mouse (Matsusue et al., 2003). Thus, fsp27 may be the target gene resulting in exacerbation of steatosis by rosiglitazone. However, recent studies demonstrated that thiazolidinedione derivatives attenuate typical symptoms in a model of nonalcoholic steatohepatitis (Belfort et al., 2006; Lang, 2007). Pioglitazone improved hepatic inflammation, decreased the fibrogenic genes, *collagen I* and *TGFβ1* mRNA and decreased hepatic TG levels (Leclercq et al., 2007; Uto et al., 2005). Thus, the function of PPARγ activation in this model appears distinct from the fatty liver models in the *ob/ob* mouse. It is noteworthy that it remains unclear whether the thiazolidinedione derivatives directly function in the nonalcoholic steatohepatitic liver. Adiponectin, elevated by thiazolidinedione, is likely to indirectly improve nonalcoholic steatohepatitis (Tilg and Hotamisligil, 2006). On the other hand, the thiazolidinedione directly affects the *ob/ob* liver that highly expresses PPARγ resulting in induction of fsp27 and the lipogenic effect. Further, the direct effect by thiazolidinedione may predominate over the indirect effects of anti-lipogenic factors such as adiponectin. More studies are needed to elucidate the effect of thiazolidinedione derivatives in the nonalcoholic steatohepatitis model.

In summary, the present study provides new pathway for hepatic TG accumulation through fsp27. The accumulation signal is independent of *de novo* lipogenesis, fatty acid uptake or VLDL export, well-known mechanisms for hepatic TG deposition and depends on the activation of PPARγ. This finding may extend beyond livers from diabetic leptin deficient and high fat-fed mice to non-alcoholic fatty liver disease (NAFLD) (Supplemental information). Therefore, elucidating the mechanism of the triglyceride accumulating effects of fsp27 might lead to potential new therapeutic opportunities for controlling triglyceride accumulation in the liver and its associated pathologies associated with NAFLD.

Experimental Procedures

Reagents

Rosiglitazone and Wy-14,643 were purchased from Alexis Biochemical and Sigma-Aldrich, respectively. Pioglitazone and L-165041 was kindly provided by Takeda Chemical Industries Co., Ltd. (Osaka, Japan) and Merck Research Laboratories (Rahway, NJ).

Subtractive screening

Ob/*ob*-PPARγ/Cre^{+} or /Cre^{-} mice were administered rosiglitazone for 3 weeks at ~ 3 mg/kg/day (Matsusue et al., 2003). For subtractive screening, total RNA was isolated from each liver by Trizol (Invitrogen), and the poly (A) RNA was prepared from total RNA with Oligotex mRNA Mini Kit (Quiagen). The PCR-based cDNA subtraction was performed by using PCR-select cDNA subtraction□ kit (Clontech).

Construction of expression and reporter plasmids

The expression vectors encoding mouse PPARα, PPARβ PPARγ and human RXRα were previously described (Matsusue et al., 2006). To create recombinant fsp27, cide a and PPARγ fusion proteins with hemagglutinin (HA)-tag, the open reading frames (ORF) of mouse *fsp27* and *cide a* were amplified by PCR from *ob/ob* mouse liver cDNA while the pSG PPARγ expression vector was used as template for amplification of the PPARγ ORF. Each ORF was cloned to pIRES-hrGFP-2a containing HA cording region (Stratagene). Following PCR primer pairs were used; fsp27; 5'-CGGGATCCAAGGATGGACT-3' and 5'-GGAATTCGTTGCAGCATCTTCAGAC-3'; *cide a*; 5'-CGGGATCCGAACAATGGAGACCGCC-3' and 5'-GGAATTCGCATGAACCAGCCTT-3'; PPARγ; 5'-ACATGCATGCGCCACCATGGTTGACACAGAGAT-3' and 5'-CCGCTCGAGCGGATACAAGTCCTTGTAGA-3'.

The transcription start site of mouse *fsp27* was determined in an earlier report (Danesch et al., 1992). The −868 (D1), −433 (D2) and −194 (D3) bp fragments from the transcriptional start site (−1) of the mouse *fsp27* promoter containing *Kpn*I and *Mlu*I sites in the 5'- and 3'-end of the primers were amplified by PCR and cloned into the luciferase reporter vector, pGL3 basic (Promega, Madison, WI). Point-mutations were introduced into the putative PPRE site in the D2 constructs by PCR-based, site-directed mutagenesis using the following two primer pairs, mut1; 5'-ACGGGAGAACGTATCACGGTACCCGTCA-3' and 5'-GTACCGTGATACGTTCTCCCGTGTCTTC-3' (mutations in the putative PPRE site are underlined), Mut2; 5'- GAAGACACGGTAGAACGGATCACGGTAC-3' and 5'-GATCCGTTCTACCGTGTCTTCGTTACC-3' (mutations in the putative PPRE site are underlined).

Northern and Western blot analysis

Northern blot analysis were performed as previously described (Matsusue et al., 2003). Open reading frame in *fsp27* or *cide a* expression vectors was used as cDNA probe. The cDNA probe for *cide b* was amplified by PCR from a mouse liver cDNA library by using gene-specific primers, and cloned into pGEM-T Easy Vector (Promega, Madison, WI). The primers used for PCR were as follows; *cide b*; 5'- GGAGTACCTTTCAGCCTTCAACC-3' and 5'-CCTTGGAAATCACAGCTCATGG. Western blot analysis were also performed as previously described (Matsusue et al., 2003).

In vitro translation and electrophoretic mobility shift assay

The *in vitro* translation and electrophoretic mobility shift assay was previously described (Matsusue et al., 2006). An oligonucleotide as probe was synthesized with the following sequences; consensus PPRE (DR1) (Juge-Aubry et al., 1997); *fsp27*/PPRE, 5'-CTGTGCCCTCTTGCCTAGTGC -3' and *aP2*/PPRE (Juge-Aubry et al., 1997), 5'-CTCTCTGGGTGAAATGTGCATTTCTG-3' along with an oligonucleotide of complementary sequence.

Production, purification, and infection of recombinant adenovirus

The recombinant adenovirus expressing mouse fsp27, cide a, PPARγ and LacZ were constructed by using the Adeno-X Expression System 2 kit (Clontech). The titer of the adenovirus was determined by adeno-X rapid titer kit (Clontech). Hepatocytes were infected by each adenovirus in no serum DMEM/F12 medium for 1 h at a dose of multiplicity of infection (MOI) described in Figure legends. *In vivo* infection, the mice (10−12-week old) were intravenously injected (tail vein) in a volume of 200 μl with 3×10^{11} infection unit of AdLacZ or Adfsp27 and killed 6 days later.

Generation and infection of the adenovirus construct expressing short hairpin RNA against fsp27

The recombinant adenovirus expressing *short hairpin RNA targeting* fsp27 were constructed by using the BLOCK-it Adenoviral RNAi Expression System (Invitrogen). The nucleotide sequence for the short hairpin RNA (shRNA) against fsp27 was designed by BLOCK-iT RNAi Designer (https://rnaidesigner.invitrogen.com/rnaiexpress/index.jsp). The finally selected sequensces are follows: fsp27 (forward); caccGGAAGGTTCGCAAAGGCATCAcgaaTGATGCCTTTGCGAACCTTCC, fsp27 (reverse); aaaaGGAAGGTTCGCAAAGGCATCAttcgTGATGCCTTTGCGAACCTTCC.

Scramble (forward); caccGCGCGCTTTGTAGGATTCGcgaaCGAATCCTACAAAGCGCGC. Scramble (reverse); aaaaGCGCGCTTTGTAGGATTCGttcgCGAATCCTACAAAGCGCGC. The procedures for the production and purification of recombinant adenovirus were in accordance with the manufacturer's instruction manual.

In vivo infection of adenovirus shRNA, the *ob/ob*-PPARγ/Cre^{-} (10−12-week old) mice were firstly administered by rosiglitazone for 3 weeks at ~ 3 mg/kg/d. The mice were intravenously injected (tail vein) in a volume of 400 μl with 1.2×10^{10} particles of Adshscram or Adshfsp27 and killed 7 days later.

Chromatin immunoprecipitation assay

Chromatin immunoprecipitation assay (ChIP assay) was performed using a Chromatin Immunoprecipitation Assay Kit (Upstate) with anti-PPARγ antibodies (H-100, SantaCruz). Fully differentiated 3T3-L1 adipocytes were incubated with or without 1 μM rosiglitazone for 3 days. A ChIP assay was also performed using crude nuclear fraction from *ob/ob* mouse liver as previously described (del Castillo-Olivares et al., 2004). Following procedures was carried out using ChIP kit as described above.

Used primers were as follows: *fsp27*/PPRE-forward, 5'-CAGACCATAAGCCACATCCATTG-3'; *fsp27*/PPRE-reverse, 5'-CACAACCCAACACTACCCAAGC-3'; *fsp27*/non-PPRE-forward, 5'-AAGAATAAGTCGGACCAAGGTGG-3'; *fsp27*/non-PPRE-reverse, 5'-GCAATCGCTCTACTCTGGCAAAG-3'; aP2/PPRE-forward (Guan et al., 2005), 5'-

ATGTCACAGGCATCTTATCCACC-3'; *aP2*/PPRE-reverse, 5'-AACCCTGCCAAAGAGACAGAGG-3'.

Measurements of TG synthesis and β-oxidation activity

The ^{14}C-labeled TG on TLC plate was detected and quantified with a BAS-2000 imaging analyzer (Fuji Photo. Film Co., Ltd.). TG synthesis and total β-oxidation activity were measured according to earlier report (Evans et al., 1992; Linden et al., 2004). The peroxisomal β-oxidation activity was measured in the presence of 4 μg/ml antimycine and 20 μg/ml rotenone to inhibit mitochondrial β-oxidation (Linden et al., 2004), while mitochondrial activity was calculated by subtracting the peroxisomal activity from total activity without antimycine and rotenone. All results are normalized by protein content and displayed as % values of AdLacZ-infected hepatocytes.

Measurement of triglyceride turnover in hepatocytes

The measurement of triglyceride turnover by ^{14}C-oleate/BSA complex was carried out according to an earlier report (Magnusson et al., 2006). Hepatocytes were seeded at a density of 5.0×10^5/well on collagen-coated 6-well plates and were incubated with 0.5 μCi/well of ^{14}C-oleate/BSA in 1 ml of no serum DMEM/F12 medium for 24 h. After washing two times with PBS, the hepatocytes were infected by each adenovirus in 500 μl of no serum DMEM/F12 medium for 1 h and incubated with 20 μM triacsin C (BioMol, Plymouth Meeting, PA), an inhibitor of acyl co-enzyme A synthetase, to inhibit new triglyceride synthesis. At the indicated times, the ^{14}C-labeled TG was quantified as described above.

Acknowledgements

This work was supported by a grant from ONO Medical Research Foundation (K.M.), Takeda Science Foundation (K.M.), Suzuken Memorial Foundation (K.M.), a Grant-in-Aid for Young Scientists (B) from the Ministry of Education, Culture, Sports, Science and Technology of Japan (K.M., 17790079) and the National Cancer Institute Intramural Research Program (F.G.). We are grateful to Takeda Chemical Industries (Osaka, Japan) for providing the pioglitazone used in this study.

References

Bedoucha M, Atzpodien E, Boelsterli UA. Diabetic KKAy mice exhibit increased hepatic PPARgamma1 gene expression and develop hepatic steatosis upon chronic treatment with antidiabetic thiazolidinediones. J. Hepatol 2001;35:17–23. [PubMed: 11495036]

Belfort R, Harrison SA, Brown K, Darland C, Finch J, Hardies J, Balas B, Gastaldelli A, Tio F, Pulcini J, et al. A placebo-controlled trial of pioglitazone in subjects with nonalcoholic steatohepatitis. N. Engl. J. Med 2006;355:2297–2307. [PubMed: 17135584]

Brasaemle DL, Rubin B, Harten IA, Gruia-Gray J, Kimmel AR, Londos C. Perilipin A increases triacylglycerol storage by decreasing the rate of triacylglycerol hydrolysis. J. Biol. Chem 2000;275:38486–38493. [PubMed: 10948207]

Chen Z, Guo K, Toh SY, Zhou Z, Li P. Mitochondria localization and dimerization are required for CIDE-B to induce apoptosis. J. Biol. Chem 2000;275:22619–22622. [PubMed: 10837461]

Danesch U, Hoeck W, Ringold GM. Cloning and transcriptional regulation of a novel adipocyte-specific gene, FSP27. CAAT-enhancer-binding protein (C/EBP) and C/EBP-like proteins interact with sequences required for differentiation-dependent expression. J. Biol. Chem 1992;267:7185–7193. [PubMed: 1339452]

del Castillo-Olivares A, Campos JA, Pandak WM, Gil G. The role of alpha1-fetoprotein transcription factor/LRH-1 in bile acid biosynthesis: a known nuclear receptor activator that can act as a suppressor of bile acid biosynthesis. J. Biol. Chem 2004;279:16813–16821. [PubMed: 14766742]

Evans AJ, Sawyez CG, Wolfe BM, Huff MW. Lipolysis is a prerequisite for lipid accumulation in HepG2 cells induced by large hypertriglyceridemic very low density lipoproteins. J. Biol. Chem 1992;267:10743–10751. [PubMed: 1587849]

Gervois P, Fruchart JC, Staels B. Drug Insight: mechanisms of action and therapeutic applications for agonists of peroxisome proliferator-activated receptors. Nat. Clin. Pract. Endocrinol. Metab 2007;3:145–156. [PubMed: 17237841]

Guan HP, Ishizuka T, Chui PC, Lehrke M, Lazar MA. Corepressors selectively control the transcriptional activity of PPARgamma in adipocytes. Genes Dev 2005;19:453–461. [PubMed: 15681609]

Ibdah JA, Paul H, Zhao Y, Binford S, Salleng K, Cline M, Matern D, Bennett MJ, Rinaldo P, Strauss AW. Lack of mitochondrial trifunctional protein in mice causes neonatal hypoglycemia and sudden death. J. Clin. Invest 2001;107:1403–1409. [PubMed: 11390422]

Inohara N, Koseki T, Chen S, Wu X, Nunez G. CIDE, a novel family of cell death activators with homology to the 45 kDa subunit of the DNA fragmentation factor. Embo J 1998;17:2526–2533. [PubMed: 9564035]

Inoue M, Ohtake T, Motomura W, Takahashi N, Hosoki Y, Miyoshi S, Suzuki Y, Saito H, Kohgo Y, Okumura T. Increased expression of PPARgamma in high fat diet-induced liver steatosis in mice. Biochem. Biophys. Res. Commun 2005;336:215–222. [PubMed: 16125673]

Juge-Aubry C, Pernin A, Favez T, Burger AG, Wahli W, Meier CA, Desvergne B. DNA binding properties of peroxisome proliferator-activated receptor subtypes on various natural peroxisome proliferator response elements. Importance of the 5'-flanking region. J. Biol. Chem 1997;272:25252–25259. [PubMed: 9312141]

Lang L. Pioglitazone trial for NASH: results show promise. Gastroenterology 2007;132:836–838. [PubMed: 17383411]

Leclercq IA, Lebrun VA, Starkel P, Horsmans YJ. Intrahepatic insulin resistance in a murine model of steatohepatitis: effect of PPARgamma agonist pioglitazone. Lab. Invest 2007;87:56–65. [PubMed: 17075577]

Liang L, Zhao M, Xu Z, Yokoyama KK, Li T. Molecular cloning and characterization of CIDE-3, a novel member of the cell-death-inducing DNA-fragmentation-factor (DFF45)-like effector family. Biochem. J 2003;370:195–203. [PubMed: 12429024]

Lin SC, Li P. CIDE-A, a novel link between brown adipose tissue and obesity. Trends Mol. Med 2004;10:434–439. [PubMed: 15350895]

Linden D, William-Olsson L, Rhedin M, Asztely AK, Clapham JC, Schreyer S. Overexpression of mitochondrial GPAT in rat hepatocytes leads to decreased fatty acid oxidation and increased glycerolipid biosynthesis. J. Lipid Res 2004;45:1279–1288. [PubMed: 15102885]

Magnusson B, Asp L, Bostrom P, Ruiz M, Stillemark-Billton P, Linden D, Boren J, Olofsson SO. Adipocyte differentiation-related protein promotes fatty acid storage in cytosolic triglycerides and inhibits secretion of very low-density lipoproteins. Arterioscler. Thromb. Vasc. Biol 2006;26:1566–1571. [PubMed: 16627799]

Mansen A, Guardiola-Diaz H, Rafter J, Branting C, Gustafsson JA. Expression of the peroxisome proliferator-activated receptor (PPAR) in the mouse colonic mucosa. Biochem. Biophys. Res. Commun 1996;222:844–851. [PubMed: 8651933]

Matsusue K, Haluzik M, Lambert G, Yim SH, Gavrilova O, Ward JM, Brewer B Jr. Reitman ML, Gonzalez FJ. Liver-specific disruption of PPARgamma in leptin-deficient mice improves fatty liver but aggravates diabetic phenotypes. J. Clin. Invest 2003;111:737–747. [PubMed: 12618528]

Matsusue K, Miyoshi A, Yamano S, Gonzalez FJ. Ligand-activated PPARbeta efficiently represses the induction of LXR-dependent promoter activity through competition with RXR. Mol. Cell. Endocrinol 2006;256:23–33. [PubMed: 16806672]

Memon RA, Tecott LH, Nonogaki K, Beigneux A, Moser AH, Grunfeld C, Feingold KR. Up-regulation of peroxisome proliferator-activated receptors (PPAR-alpha) and PPAR-gamma messenger ribonucleic acid expression in the liver in murine obesity: troglitazone induces expression of PPAR-gamma-responsive adipose tissue-specific genes in the liver of obese diabetic mice. Endocrinology 2000;141:4021–4031. [PubMed: 11089532]

Puri V, Konda S, Ranjit S, Aouadi M, Chawla A, Chouinard M, Chakladar A, Czech MP. Fat-specific Protein 27, a Novel Lipid Droplet Protein That Enhances Triglyceride Storage. J. Biol. Chem 2007;282:34213–34218. [PubMed: 17884815]

Rosen ED, Hsu CH, Wang X, Sakai S, Freeman MW, Gonzalez FJ, Spiegelman BM. C/EBPalpha induces adipogenesis through PPARgamma: a unified pathway. Genes Dev 2002;16:22–26. [PubMed: 11782441]

Schadinger SE, Bucher NL, Schreiber BM, Farmer SR. PPARgamma2 regulates lipogenesis and lipid accumulation in steatotic hepatocytes. Am. J. Physiol. Endocrinol. Metab 2005;288:E1195–1205. [PubMed: 15644454]

Simon DM, Arikan MC, Srisuma S, Bhattacharya S, Tsai LW, Ingenito EP, Gonzalez F, Shapiro SD, Mariani TJ. Epithelial cell PPAR[gamma] contributes to normal lung maturation. Faseb J 2006;20:1507–1509. [PubMed: 16720732]

Thomas J, Debeer LJ, Mannaerts GP, De Schepper PJ. Mitochondrial and peroxisomal fatty acid oxidation in liver homogenates from control and clofibrate-treated rats [proceedings]. Arch. Int. Physiol. Biochim 1979;87:209–210. [PubMed: 92279]

Tilg H, Hotamisligil GS. Nonalcoholic fatty liver disease: Cytokine-adipokine interplay and regulation of insulin resistance. Gastroenterology 2006;131:934–945. [PubMed: 16952562]

Tomoda H, Igarashi K, Cyong JC, Omura S. Evidence for an essential role of long chain acyl-CoA synthetase in animal cell proliferation. Inhibition of long chain acyl-CoA synthetase by triacsins caused inhibition of Raji cell proliferation. J. Biol. Chem 1991;266:4214–4219. [PubMed: 1999415]

Tontonoz P, Hu E, Graves RA, Budavari AI, Spiegelman BM. mPPAR gamma 2: tissue-specific regulator of an adipocyte enhancer. Genes Dev 1994;8:1224–1234. [PubMed: 7926726]

Uto H, Nakanishi C, Ido A, Hasuike S, Kusumoto K, Abe H, Numata M, Nagata K, Hayashi K, Tsubouchi H. The peroxisome proliferator-activated receptor-gamma agonist, pioglitazone, inhibits fat accumulation and fibrosis in the livers of rats fed a choline-deficient, l-amino acid-defined diet. Hepatol. Res 2005;32:235–242. [PubMed: 16085455]

Viswakarma N, Yu S, Naik S, Kashireddy P, Matsumoto K, Sarkar J, Surapureddi S, Jia Y, Rao MS, Reddy JK. Transcriptional regulation of mitochondrial cell death-inducing DNA fragmentation factor alpha -like effector A (Cidea) in mouse liver by PPARalpha and PPARgamma. J. Biol. Chem 2007;282:18613–18624. [PubMed: 17462989]

Vivat-Hannah V, Bourguet W, Gottardis M, Gronemeyer H. Separation of retinoid X receptor homo- and heterodimerization functions. Mol. Cell. Biol 2003;23:7678–7688. [PubMed: 14560013]

Williams PM, Chang DJ, Danesch U, Ringold GM, Heller RA. CCAAT/enhancer binding protein expression is rapidly extinguished in TA1 adipocyte cells treated with tumor necrosis factor. Mol. Endocrinol 1992;6:1135–1141. [PubMed: 1508226]

Zhou Z, Yon Toh S, Chen Z, Guo K, Ng CP, Ponniah S, Lin SC, Hong W, Li P. Cidea-deficient mice have lean phenotype and are resistant to obesity. Nat. Genet 2003;35:49–56. [PubMed: 12910269]

Supplementary Material

Refer to Web version on PubMed Central for supplementary material.

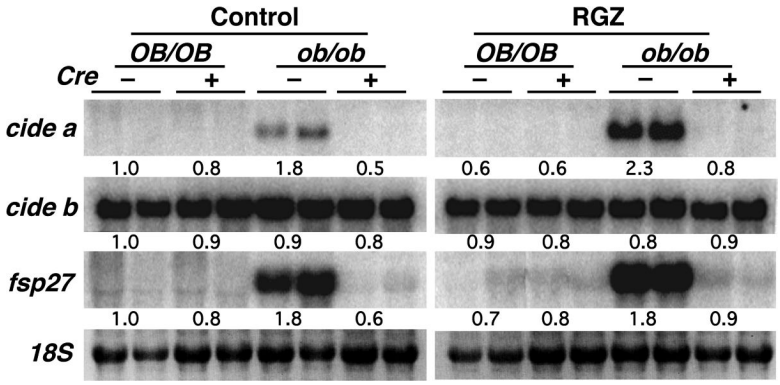

Figure 1.

The expression of *cide a* and *fsp27* genes depends on the hepatic PPARγ and fatty liver formation, but not *cide b*. Northern blot analysis was performed on total RNA (10 μg) from two mice. Rosiglitazone at 3 mg/kg/day was fed to mice for 3 weeks. Control, diet without rosiglitazone; RGZ, diet containing rosiglitazone; *OB/OB*, normal genetic background mice; *ob/ob*; leptin-deficient mice.

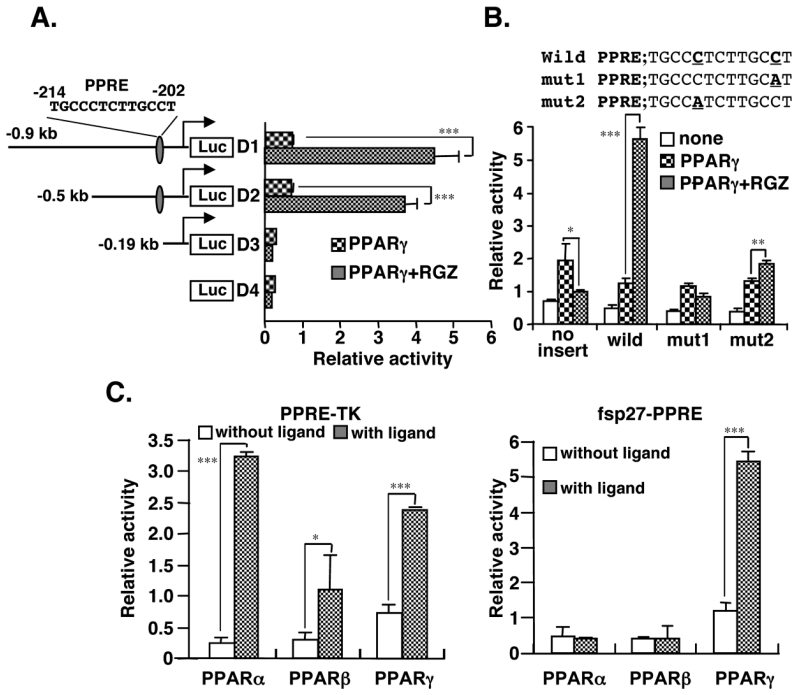

Figure 2.

Identification of a functional peroxisome proliferator-activated receptor response element (PPRE) in the mouse *fsp27* promoter. (A) Ligand-activated PPARγ induces the promoter activity of *fsp27* gene through a putative PPRE. HEK293 cells were transfected with serially deleted *fsp27* luciferase reporter plasmids and an pSG-PPARγ expression vector. Following 6 hr after transfection, the medium was changed to fresh medium containing 1 μM rosiglitazone or DMSO. The cells were harvested at 48 hr after transfection and luciferase activity was measured. (B) HEK293 cells were transfected with the reporter plasmids containing a point-mutation of a putative PPRE sequence in the *fsp27* promoter. In the mut1 and 2 plasmids, a cytosine base (bold) replaced an adenine base (bold) in the putative PPRE sequence in the D2 plasmid as indicated in upper panel. (C) PPARγ-specific activation of the *fsp27* promoter activity. HEK293 cells were transfected with the thymidine kinase promoter (TK) including the consensus PPRE sequence promoter as positive control or *fsp27* promoter luciferase plasmids (D2 plasmid in A) and each PPAR isoform expression vector. Following 6 hr after transfection, the cells were treated with each specific ligand; PPARα, 50 μM Wy-14,643; PPARβ, 0.5 μM L-165041; PPARγ, 1μM rosiglitazone. Data are mean ± SE from three independent experiments. Significant differences from control (without ligand): *p<0.05, **p<0.01, *** p<0.001.

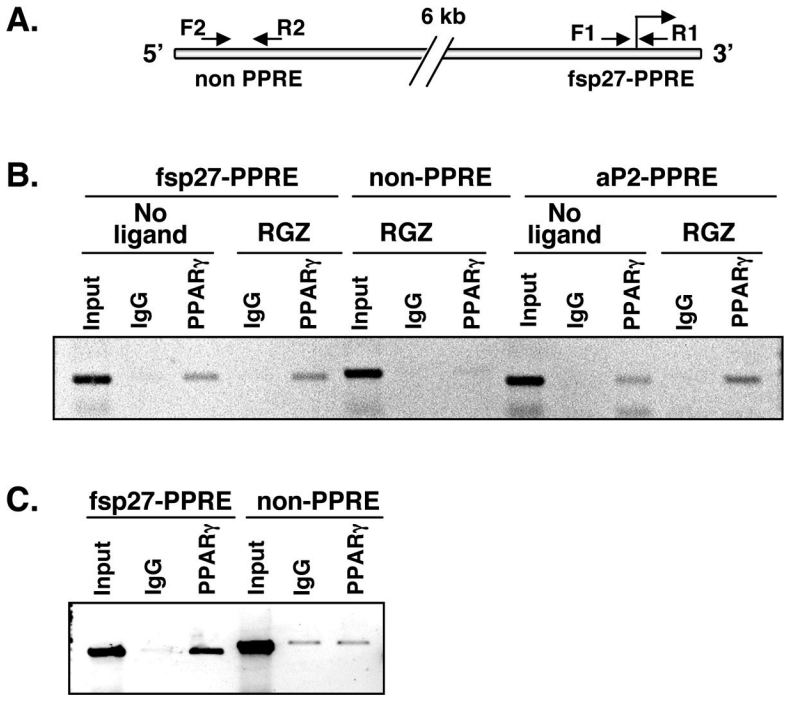

Figure 3.

Endogenous PPARγ associates with fsp27-PPRE. (A) The positions of primers (arrows) relative to the PPRE of the *fsp27* promoter are shown. The PPRE located in *fsp27* promoter was amplified by the F1 and R1 primer sets (fsp27-PPRE). PPRE in the 5'upstream of the *aP2* gene was used as a positive control (aP2-PPRE). Primer sets (F2 and R2) that are located > 6 kb upstream of the fsp27-PPRE (non PPRE) were also used as a negative control. (B) Endogenous PPARγ in 3T3-L1 adipocytes binds to *fsp27*-PPRE. Fully differentiated adipocytes were cultured with or without 1 μM rosiglitazone (RGZ) for 48 hr and the soluble chromatin from the cells was prepared as described in Material and Methods. IgG, rabbit control IgG; PPARγ, rabbit anti PPARγ IgG. (C) Endogenous PPARγ in *ob/ob* mouse liver binds to *fsp27*-PPRE. Input; Genomic DNA from the chromatin before immunoprecipitation as the positive control for PCR.

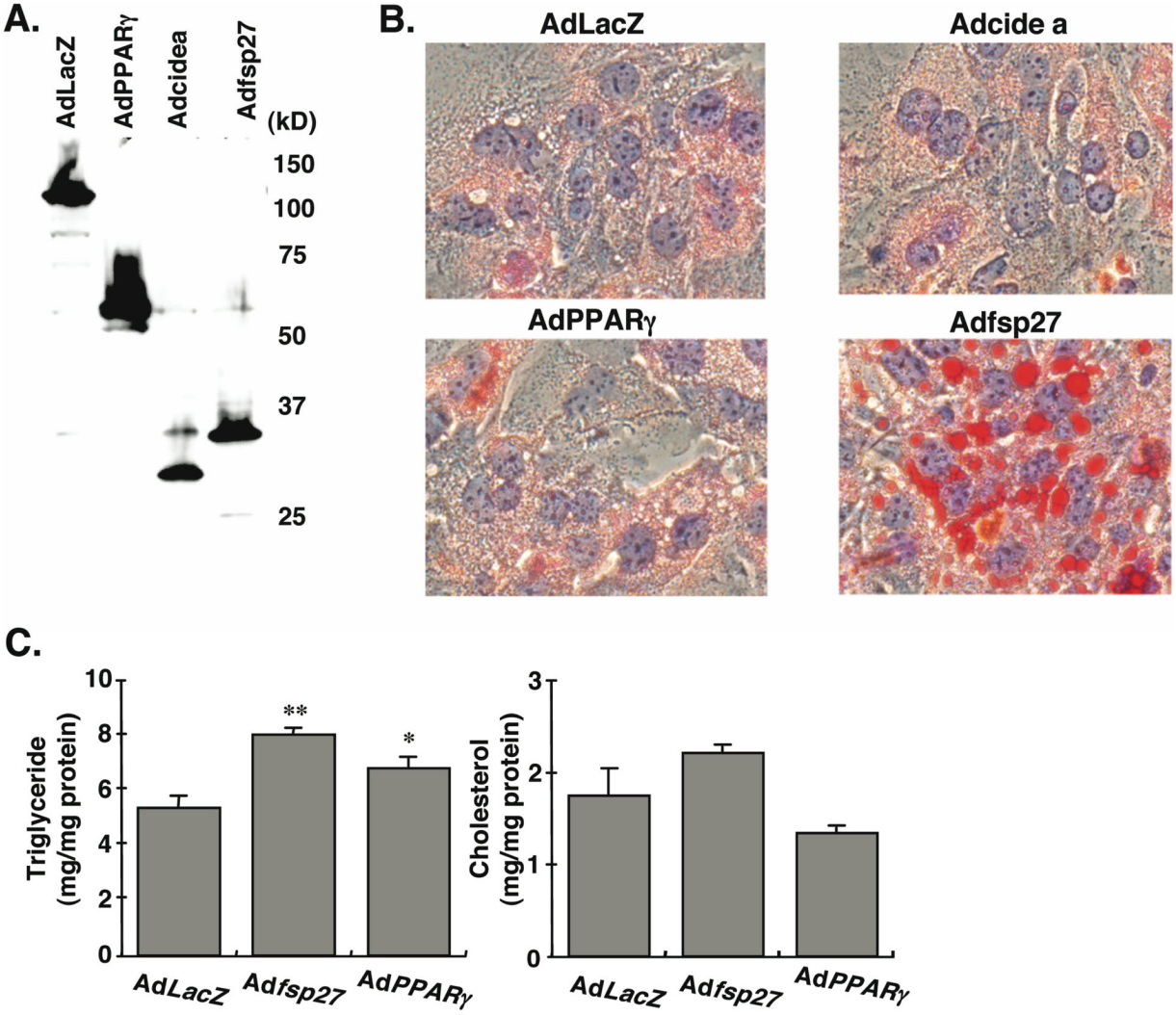

Figure 4.

Overexpression of fsp27 protein in mouse primary hepatocytes leads to triglyceride accumulation. (A) Verification of HA-fused proteins expressed by recombinant adenovirus vectors in mouse primary hepatocytes. The hepatocytes from C57/BL mice were infected with Adfsp27, cidea, PPARγ and LacZ at 500 MOI. Following 2 days after the infection, the lysates from each hepatocyte were subjected to Western blot analysis by HA antibody. (B) Oil Red O staining in adenovirus-infected hepatocytes. The hepatocytes from C57/BL mice were infected with Adfsp27, Adcidea, AdPPARγ and AdLacZ at 500 MOI. Following 3 days after infection, each hepatocyte was stained with Oil Red O. The nuclei were also counterstained with hematoxylin. (C) Total triglyceride and cholesterol contents in adenovirus-infected hepatocytes. The infection condition is same as described above. Data are mean ± SE from three independent experiments. Significant differences compared to AdLacZ-infected hepatocytes: *, $p < 0.05$, **, $p < 0.01$.

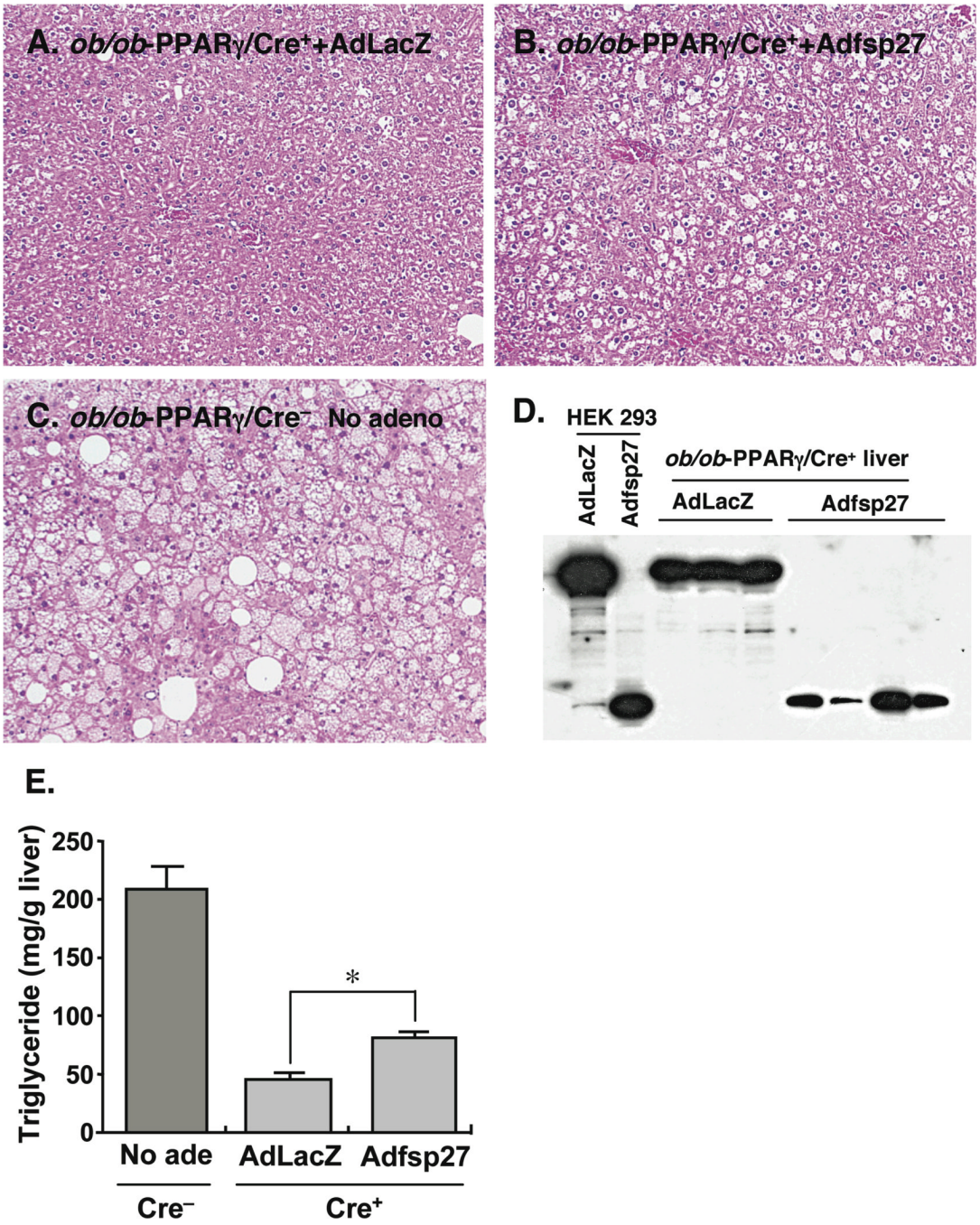

Figure 5.

Overexpression of fsp27 protein in *ob/ob* liver lacking PPARγ restores triglyceride accumulation. *Ob/ob*-PPARγ/Cre^{+} mice were treated with pioglitazone for 3 weeks and then injected with AdLacZ (A) and Adfsp27 (B). The mice were maintained on 0.01% pioglitazone for another 6 days. Likewise, *ob/ob*-PPARγ/Cre^{-} mice were treated with pioglitazone and without adenovirus infection as a positive control. HE staining was performed on liver sections from each mouse line/treatment. The Adfsp27-infected ob/ob-PPARγ/Cre+ mice exhibited fatty liver, as revealed by vacuolated hepatocytes, while the livers of AdLacZ-infected ob/ob-PPARγ /Cre+ mice remained unchanged. (C) Uninfected ob/ob-PPARγ/Cre− mice are shown for comparison Verification of LacZ-HA and fsp27-HA proteins expressed by recombinant

adenovirus vectors in *ob/ob*-PPARγ/Cre^{+} mouse liver (D). The cell lysates of livers as shown above were subjected to Western blot analysis using the HA antibody. The lysate from HEK 293 cells, infected with AdLacZ and Adfsp27, was used as positive control. (E). The livers from mice as shown above were also used for the measurement of hepatic triglyceride contents The mouse number for each group as follows; *ob/ob*-PPARγ/Cre^{-}; 5 (Male 2; Female 3), AdLacZ-infected *ob/ob*-PPARγ/Cre^{+}; 3 (Male 3), Adfsp27-infected *ob/ob*-PPARγ/Cre^{+}; 4 (Male 4). Data are mean ± SE. Significant differences compared to AdLacZ-infected hepatocytes: *, $p < 0.01$

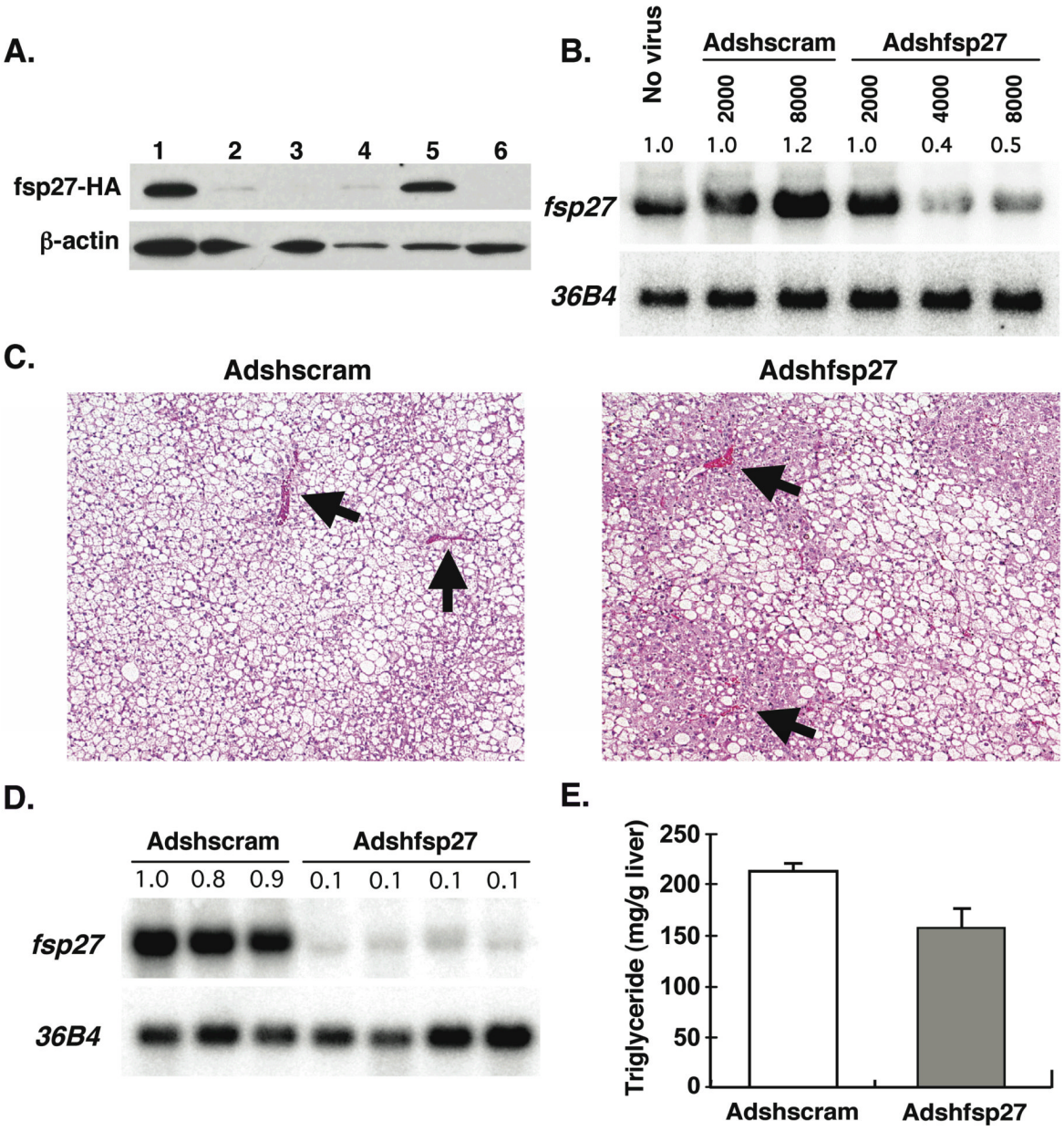

Figure 6.

Knockdown of fsp27 in *ob/ob*-PPARγ/Cre^{-} liver partially decreases hepatic triglyceride. Identification of efficient fsp27-shRNA sequences (A) Fsp27-HA expression plasmid was co-transfected to HEK293 cells with following plasmids; fsp27-shRNA sequence 1 (lane 2), sequence 2 (lane 3) and sequence 3 (lane 4) plasmids or control scramble sequence plasmid (lane 5). Following 3 days after transfection, cell lysates were prepared from each cell and subjected to Western blot analysis by HA-antibody. The fsp27-HA expression plasmid alone (lane 1) or no plasmid (lane 6) was also examined. (B) Effect of Adshfsp27 on the *fsp27* mRNA expressed constitutively in 3T3-L1 adipocytes Recombinant adenovirus expressing short hairpin RNA targeting fsp27 (Adshfsp27) or control scramble (Adshscram) were infected to 3T3-L1 adipocytes. Total RNA from each cell infected with different MOI was subjected to Northern blot analysis. (C) HE staining was performed for liver sections from each mouse line/treatment. *Ob/ob*-PPARγ/Cre^{-} mice were treated with rosiglitazone for 3 weeks and then

injected with Adshscram and Adshfsp27. The mice were maintained on rosiglitazone for another 7 days. (D) Effect of Adshfsp27 on the *fsp27* mRNA expressed constitutively in Adshfsp27- or Adscram-injected livers. Northern blot analysis was performed on total RNA (10 μg) from livers of each mouse. (E) The livers as shown above were also used for the measurement of hepatic triglyceride contents. The mouse number for each group as follows; Adshscram-injected mice; 3 (Male 3), Adshfsp27-injected mice; 4 (Male 4). Data are mean ± SE.

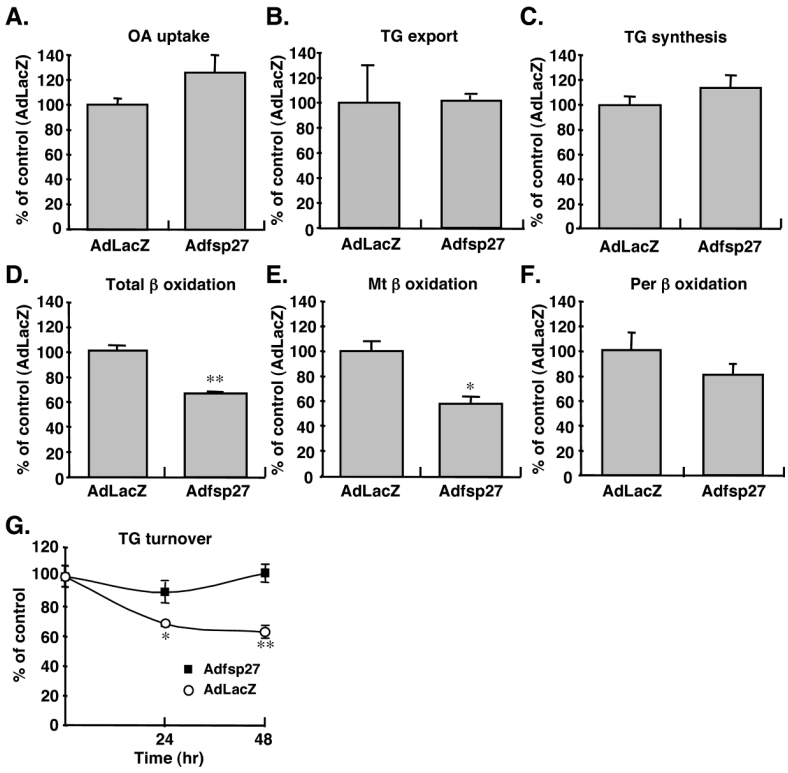

Figure 7.

Overexpression of fsp27 in hepatocytes represses mitochondrial β-oxidation activity and reduces triglyceride turnover. Mouse primary hepatocytes were incubated with 500 MOI of AdLacZ or fsp27 for 3 days and then with ^{14}C-oleate/BSA complexes. (A) ^{14}C-oleate uptake into hepatocytes. (B) Export of ^{14}C-oleate-incorporated triglyceride (TG) into medium. (C) TG synthesis from ^{14}C-oleate. (D) Total β-oxidation. (E) Mitochondrial (Mt) β-oxidation activity. (F) Peroxisomal (Per) β-oxidation activity. The per β-oxidation activity was measured in the presence of 4 μg/ml antimycine and 20 μg/ml rotenone to inhibit Mt β-oxidation activity. The results (A-F) are normalized by protein content and displayed as % values of AdLacZ-infected hepatocytes. (G) Turnover of triglyceride in hepatocytes expressing fsp27. Mouse primary hepatocytes were incubated with ^{14}C-oleate/BSA complex for 24 hr and then with 500 MOI of AdLacZ or fsp27 in the presence of 20 μM triacsin C. The results are normalized by protein content and displayed as % values of time 0 hr. Data are mean ± SE from three independent experiments. Significant differences compared to AdLacZ-infected hepatocytes: *, $p < 0.01$, **, $p < 0.001$.